



HAL
open science

Optimization of Course Locations in Fiber-Placed Panels for General Fiber Angle Distributions

Adriana W. Blom, Mostafa M. Abdalla, Zafer Gürdal

► **To cite this version:**

Adriana W. Blom, Mostafa M. Abdalla, Zafer Gürdal. Optimization of Course Locations in Fiber-Placed Panels for General Fiber Angle Distributions. *Composites Science and Technology*, 2010, 70 (4), pp.564. 10.1016/j.compscitech.2009.12.003 . hal-00615117

HAL Id: hal-00615117

<https://hal.science/hal-00615117>

Submitted on 18 Aug 2011

HAL is a multi-disciplinary open access archive for the deposit and dissemination of scientific research documents, whether they are published or not. The documents may come from teaching and research institutions in France or abroad, or from public or private research centers.

L'archive ouverte pluridisciplinaire **HAL**, est destinée au dépôt et à la diffusion de documents scientifiques de niveau recherche, publiés ou non, émanant des établissements d'enseignement et de recherche français ou étrangers, des laboratoires publics ou privés.

Accepted Manuscript

Optimization of Course Locations in Fiber-Placed Panels for General Fiber Angle Distributions

Adriana W. Blom, Mostafa M. Abdalla, Zafer Gürdal

PII: S0266-3538(09)00428-X
DOI: [10.1016/j.compscitech.2009.12.003](https://doi.org/10.1016/j.compscitech.2009.12.003)
Reference: CSTE 4583

To appear in: *Composites Science and Technology*

Received Date: 3 February 2009
Revised Date: 1 December 2009
Accepted Date: 6 December 2009

Please cite this article as: Blom, A.W., Abdalla, M.M., Gürdal, Z., Optimization of Course Locations in Fiber-Placed Panels for General Fiber Angle Distributions, *Composites Science and Technology* (2009), doi: [10.1016/j.compscitech.2009.12.003](https://doi.org/10.1016/j.compscitech.2009.12.003)

This is a PDF file of an unedited manuscript that has been accepted for publication. As a service to our customers we are providing this early version of the manuscript. The manuscript will undergo copyediting, typesetting, and review of the resulting proof before it is published in its final form. Please note that during the production process errors may be discovered which could affect the content, and all legal disclaimers that apply to the journal pertain.



Optimization of Course Locations in Fiber-Placed Panels for General Fiber Angle Distributions

Adriana W. Blom ^{a,*} Mostafa M. Abdalla ^a Zafer Gürdal ^a

^a*Aerospace Structures, Delft University of Technology, Kluyverweg 1, 2629HS Delft, The Netherlands*

Abstract

Fiber-reinforced composites are usually designed using constant fiber orientation in each ply. In certain cases, however, a varying fiber angle might be favorable for structural performance. This possibility can be fully utilized using tow placement technology. Because of the fiber angle variation, tow-placed courses may overlap and ply thickness will build up on the surface. This thickness build-up affects manufacturing time, structural response, and surface quality of the finished product.

This paper will present a method for designing composite plies with varying fiber angles with composite plates or panels. The thickness build-up within a ply is predicted as function of ply angle variation using a streamline analogy. It is found that the thickness build-up is not unique and depends on the chosen start locations of fiber courses. Optimal fiber courses are formulated in terms of minimizing the maximum ply thickness, maximizing surface smoothness or combining these objectives with and without periodic boundary conditions.

Key words: A. Laminate, A. Structural composite, A. Fibers, E. Fiber placement, Optimization

1 Introduction

In industry fiber-reinforced composites are usually designed using a constant fiber orientation in each ply. The fiber angles in these laminates are typically 0, 90, and ± 45 degrees. Traditionally the choice of these lay-ups was motivated by manufacturability, while nowadays lay-ups with changing or even non-conventional fiber angles are avoided because of the lack of allowables. However, research on composites with a varying in-plane fiber orientation has shown that variable stiffness can be beneficial for structural performance [1–17], because variable-stiffness laminates are able to redistribute the loading more efficiently than constant-stiffness laminates. In most cases curvilinear fiber paths manufactured by tow placement are used to construct the variable-stiffness laminates [4, 5, 9–11, 15, 18–20]. Jegley, Tatting and Gürdal [9–11] designed variable-stiffness flat plates with holes and demonstrated their effectiveness by building and testing several specimens.

Due to fiber angle variation, a tow-placed shell typically exhibits gaps and/or overlaps between adjacent courses and ply thickness will change along the surface [9–11, 18]. The amount of gap/overlap affects structural response, manufacturing time, and surface quality of the finished product.

This paper presents a method for designing composite plies which have spatially varying fiber angles. Since fiber-reinforced laminates usually consist of multiple plies, optimizations for specific

* Corresponding author.

Email address: A.W.Blom@TUDelft.nl (Adriana W. Blom).

loading conditions result in multiple plies with different fiber angle distributions. The fiber angle distribution per ply can be used as a direct input for the optimization, as is done by most researchers so far [1–20], or it can be obtained in a post processing step, where an optimum laminate stiffness distribution is approximated as closely as possible, as described by Setoodeh [21]. In these optimizations the ply thickness is usually assumed to be constant, without taking into consideration manufacturing issues. In the current paper the fiber angle distribution per ply is assumed given, being one of the plies within an optimized laminate. The thickness build-up is predicted as function of ply angle variation using a streamline analogy. It is found that the thickness build-up is not unique and depends on the chosen start locations of fiber courses. Optimal distributions of fiber courses are formulated in terms of minimizing the maximum ply thickness or maximizing surface smoothness, either with or without periodic boundary conditions. Subsequently the discrete thickness build-up resulting from the tow-placement process can be determined based on the streamline distribution. Results will be compared to the smeared thickness approximation. An overview of the analysis sequence is given in Fig. 1. Finally, a number of applications for the developed methods and suggestions for future research are given.

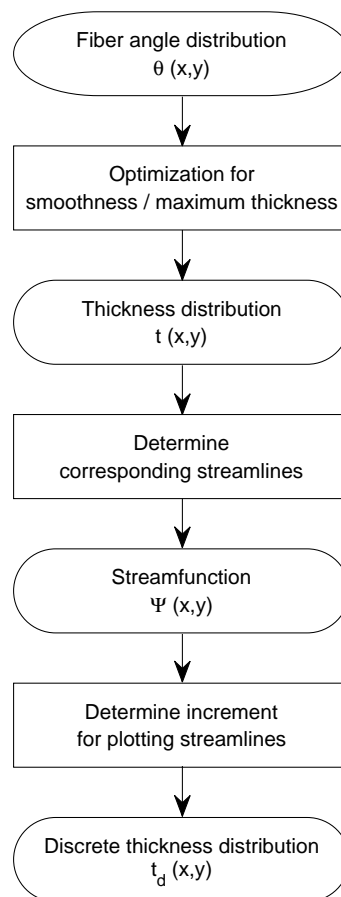


Fig. 1. Analysis sequence

2 Streamline Analogy

For the construction of discrete fiber paths a streamline analogy is being used. For this application each streamline represents the centerline of a course, or if the course width is made infinitely small

each streamline will represent a single fiber. Mathematically a streamline is represented by a stream function

$$\Psi(x, y) = C \quad (1)$$

which connects all the points with a constant value C . For a given fiber angle distribution $\theta(x, y)$, the streamlines can be found by solving the following partial differential equation:

$$\begin{aligned} \frac{d\Psi}{ds} &= \frac{\partial\Psi}{\partial x} \frac{dx}{ds} + \frac{\partial\Psi}{\partial y} \frac{dy}{ds} \\ &= \Psi_{,x} \cos \theta + \Psi_{,y} \sin \theta = 0 \end{aligned} \quad (2)$$

A unique solution for the stream function (and thus the location of the stream lines) depends on the boundary conditions. Before seeking a solution to the stream function, additional considerations relevant to the physical representation of the fiber paths are in order.

As stated earlier, the streamlines represent the central path of a finite width course. Unless the streamlines are parallel, the successive courses will always overlap each other when no gaps are allowed between them (or alternatively, the gaps will form between the passes if two successive finite width passes are not allowed to overlap). The amount of overlap depends on the distance between the course centerlines. If the distance is decreased, then the overlap area is increased. Although in reality these overlaps are discrete, a first approximation to the amount of overlap could be made by smearing out this discrete overlap to form a continuous thickness distribution. In this case, the smeared thickness, t , will be inversely proportional to the distance between adjacent courses, which can be explained as follows. If a number of N courses with a given width, w , and thickness has a fixed volume V , and if these successive courses are placed closer than the width of the courses, then the total width covered is less than $N \cdot w$, and the thickness has to be increased in order to maintain the same material volume V .

When the distance between two streamlines is $|dn|$, then $t \propto 1/|dn|$ (as explained above). Since $\Psi_{,n} = d\Psi/dn$ and $d\Psi$ between two streamlines is constant according to Eq. (1) the thickness t will be proportional to $\Psi_{,n}$ as follows:

$$t \propto \frac{1}{|dn|} = \frac{1}{d\Psi/\Psi_{,n}} = \frac{\Psi_{,n}}{d\Psi} \propto \Psi_{,n} \quad (3)$$

If $d\Psi$ is assumed to be a unity, then $t = \Psi_{,n}$, which can be used to derive a direct correlation between the thickness distribution and the fiber angle variation (see Appendix A):

$$-\bar{s}\bar{\nabla}(\ln t) = \bar{n}\bar{\nabla}\theta \quad (4)$$

in which \bar{s} and \bar{n} represent the tangent and normal vectors to a streamline, respectively, as shown in Fig. 2. The physical explanation of Eq. (4) is that the change in thickness along a streamline depends on the change of the fiber orientation perpendicular to that streamline. Since both vectors \bar{s} and \bar{n} depend on the given fiber angle distribution $\theta(x, y)$, the only unknown in Eq. (4) is the thickness. Hence, the thickness can now be determined by solving this equation, but since it is a differential equation boundary conditions are needed in order to obtain a unique solution. In accordance with streamline theory, boundary conditions are only needed at the inflow boundary, where the inflow boundary is arbitrarily defined by:

$$\bar{s} \cdot \bar{N} \leq 0 \quad (5)$$

where \bar{s} is the vector tangent to the streamline and \bar{N} is the outward normal vector to the boundary, as shown in Fig. 2. By changing the thickness at the inflow boundary, the thickness distribution inside the domain and at the outflow boundaries will change.

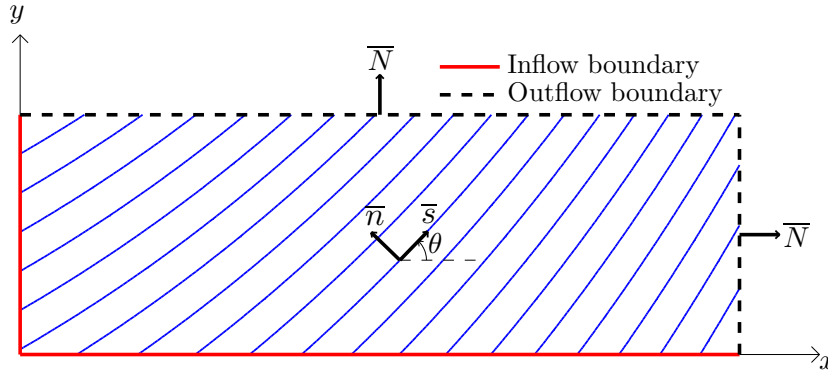


Fig. 2. Streamline definitions

3 Determining Boundary Conditions

There exist an infinite number of possible boundary conditions for which the thickness distribution associated with the streamlines can be found, but the most difficult part is to find the ones that are physically sensible for the problem in hand. In this paper the boundary conditions are established such that they fulfill a certain optimality condition. The optimality conditions to be demonstrated in this paper are minimization of maximum thickness, maximization of smoothness, and a combination of these two. In addition, constraints such as periodicity of the boundary conditions can be enforced as well.

3.1 General Solution

By using the following change of variables: $\tau = \ln t$, Eq. (4) becomes:

$$-\bar{s}\nabla\tau = \bar{n}\nabla\theta \quad (6)$$

The above equation is solved numerically by discretizing the derivatives, so that it is written as:

$$[M]\bar{\tau} = \bar{B} \quad (7)$$

where $[M]$ is the matrix that represents the left hand side of Eq. (6), $\bar{\tau}$ is the vector that represents τ at every grid point and \bar{B} is the vector that represents the right hand side of Eq. (6), as well as the boundary conditions. If the thickness at the inflow boundaries is assumed to be equal to one everywhere ($\tau = \ln t = \ln 1 = 0$), a nominal solution can be found for $\bar{\tau}$, which will be referred to as $\bar{\tau}_0$. A general solution of Eq. (7) can be expressed as:

$$\bar{\tau} = \bar{\tau}_0 + [T]\bar{\tau}_{in} \quad (8)$$

where each column j in matrix $[T]$ represents the influence of boundary grid point j on the thickness distribution in the complete domain, while satisfying Eq. (7). Since these columns are independent of each other and since Eq. (7) is a linear equation, any linear combination of these columns also represents a solution, as given by Eq. (8). The entries in $\bar{\tau}_{in}$ all render the thickness at a single point on the inflow boundary. By substituting Eq. (8) in Eq. (7), the thickness can be optimized for one of the criteria mentioned earlier by using $\bar{\tau}_{in}$ as design variables.

Often it is desired to have at least one layer of material everywhere so that no gaps exist. Therefore it is required that the thickness over the entire domain is at least one, such that $\bar{\tau} \geq \bar{0}$ in all optimizations described below. Optimization is performed by using the optimization toolbox in Matlab [22]

3.2 Minimized Maximum Thickness

Minimizing the maximum thickness of the plate is the first optimality criterion that will be elaborated on in this paper. This criterion is relevant for judging how practical the resulting thickness distribution would be in a real life structure, as well as for determining the manufacturability of a plate with constant thickness for a given fiber angle distribution. If the thickness build-up is too severe (i.e. if one point is 100 or 1000 times thicker than the average plate thickness) it will not be practical for realistic structures.

In order to solve the min-max problem, the bound formulation as introduced by Olhoff [23] is used. This formulation introduces a new variable α , which represents the maximum thickness and which also serves as the new objective function for the minimization. Additionally, a constraint on the thickness at each grid point is being introduced so that the thickness never exceeds the minimized maximum thickness, α . Mathematically:

$$\begin{aligned} F_{min} &= \alpha \\ \text{s.t.} \quad \tau_i &\leq \alpha \quad i = 1, 2, \dots, N_g \end{aligned} \quad (9)$$

where N_g is the number of grid points. The design variables that result from the optimization are substituted in Eq. (8) and then the thickness distribution is found by changing variables again: $t_i = e^{\tau_i}$.

3.3 Maximized Smoothness

Another possible optimization objective is to maximize the smoothness of the thickness distribution of the composite panel. Although in reality the change in thickness will always be discrete due to the discrete nature of tow courses, it would still be desirable for ply drops/overlaps to be distributed throughout the panel rather than to be concentrated at particular regions. In order to achieve this objective, smoothness is defined as the norm of the rate of change of thickness.

Smoothness is maximized by minimizing the H_1 -norm of the thickness:

$$\min \quad \frac{1}{2} \bar{\tau}^T [K] \bar{\tau} \quad (10)$$

where $[K]$ is the matrix that discretizes the Laplacian. Substituting the expression for $\bar{\tau}$ (Eq. (8)) into the argument of Eq. (10) gives:

$$\frac{1}{2} \bar{\tau}^T [K] \bar{\tau} = \frac{1}{2} \bar{\tau}_0^T [K] \bar{\tau}_0 + \bar{\tau}_0^T [K] [T] \bar{\tau}_{in} + \frac{1}{2} \bar{\tau}_{in}^T [T]^T [K] [T] \bar{\tau}_{in} \quad (11)$$

The first term on the right hand side of Eq. (11) is constant, so that the objective function to be minimized is:

$$F_{min} = \frac{1}{2} \bar{\tau}_{in}^T [K_r] \bar{\tau}_{in} - \bar{f}_r \bar{\tau}_{in} \quad (12)$$

with

$$\begin{aligned} [K_r] &= [T]^T [K] [T] \\ \bar{f}_r &= -\bar{\tau}_0^T [K] [T] \end{aligned} \quad (13)$$

The minimum of Eq. (12) can be found by differentiating it and equating it to zero, so that:

$$[K_r] \bar{\tau}_{in} = \bar{f}_r \quad (14)$$

This is a linear system that can be solved for $\bar{\tau}_{in}$. However, the $[K_r]$ -matrix is one time singular and therefore one entry of $\bar{\tau}_{in}$ is given an assumed value so that the system can be solved. After the

solution is substituted in Eq. (8), a constant can be added to $\bar{\tau}$ such that the condition of $\bar{\tau} \geq 0$ is being met (this will not change the H_1 -norm, but will change the absolute value of thickness).

3.4 Combined Objective Function

Since both minimizing the maximum thickness and maximizing the smoothness are valid optimization criteria, designers might consider combining the two in order to obtain a better design. Depending on the design requirements, different weighting factors can be assigned to the individual criterion. The objective functions of Eqs. (9) and (12) can then be combined to form a new objective function:

$$F_{min} = (1 - w) \frac{\alpha}{\alpha^*} + w \frac{\frac{1}{2} \bar{\tau}_{in}^T [K_r] \bar{\tau}_{in} - \bar{f}_r \bar{\tau}_{in}}{\frac{1}{2} \bar{\tau}_{in}^{T*} [K_r] \bar{\tau}_{in}^* - \bar{f}_r \bar{\tau}_{in}^*} \quad (15)$$

In this equation w is the weighting factor that indicates the importance of the smoothness in the optimization. Furthermore the two objective functions are normalized by α^* and $\frac{1}{2} \bar{\tau}_{in}^{T*} [K_r] \bar{\tau}_{in}^* - \bar{f}_r \bar{\tau}_{in}^*$, respectively, where α^* is the smallest maximum thickness obtained from Eq. (9) and $\bar{\tau}_{in}^*$ are the design variables for maximum smoothness as obtained by Eq. (12).

3.5 Periodic Boundary conditions

The present formulation would also be valid for cylindrical shells since points on a cylindrical surface are in one to one correspondence to points on a rectangular panel. Nevertheless, an important difference exists; in the case of a cylindrical shell the solution must be periodic. When the ply angle variation is periodic, continuity in thickness is obtained by including the thickness periodicity constraints in the optimization routines described above. For periodicity in y -direction, this takes the form:

$$\tau(x_i, 0) = \tau(x_i, b) \quad 0 \leq x_i \leq l \quad (16)$$

where l is the length and b is the width of the panel.

4 Discrete Fiber Courses

Once the smeared thickness distribution is obtained through one of the optimizations described above, the corresponding stream function can be obtained by integrating $\Psi_{,n}$ over dn :

$$\begin{aligned} \Psi(x, y) &= \int \Psi_{,n} dn \\ &= \int \frac{d\Psi}{dx} \frac{dx}{dn} dn + \int \frac{d\Psi}{dy} \frac{dy}{dn} dn \\ &= \int \Psi_{,x} dx + \int \Psi_{,y} dy \end{aligned} \quad (17)$$

The derivatives of Ψ with respect to x and y can be expressed as functions of $\Psi_{,s}$ and $\Psi_{,n}$ as follows:

$$\begin{aligned} \Psi_{,x} &= \Psi_{,s} \cos \theta - \Psi_{,n} \sin \theta \\ \Psi_{,n} &= \Psi_{,s} \sin \theta + \Psi_{,n} \cos \theta \end{aligned} \quad (18)$$

Since $\Psi_{,s} = 0$ and $\Psi_{,n} = t$, the combination of Eqs. (17) and (18) will give:

$$\Psi(x, y) = - \int_0^x t(x^*, y^*) \sin \theta(x^*, y^*) dx^* + \int_0^y t(x^*, y^*) \cos \theta(x^*, y^*) dy^* \quad (19)$$

Both $t(x, y)$ and $\theta(x, y)$ are known functions, so that $\Psi(x, y)$ can be solved. By plotting the contour lines of Ψ at fixed increments the streamlines are found that could represent the centerlines of the

actual fiber courses. The constant of integration will determine the exact location of the fiber courses, which can be used for staggering in case of multiple plies with the same fiber angle distribution. Once the course centerlines are known, discrete courses can be constructed by calculating the course edges. If a point on the path centerline is defined by $\{x_c, y_c\}$ the course edges are found by:

$$\begin{aligned} x_e &= x_c \mp p \sin \theta_c \\ y_e &= y_c \pm p \cos \theta_c \end{aligned} \quad (20)$$

where p is half the total course width and θ_c is the fiber orientation angle at $\{x_c, y_c\}$, as shown in Fig. 3. When the centerline reaches the domain boundary one edge is still inside the domain and therefore the centerline is extrapolated until both edges are outside the domain boundary (e.g. the blue lines in Fig. 3). After determining the location of the course boundaries the number of layers at each point in the laminate can be found.

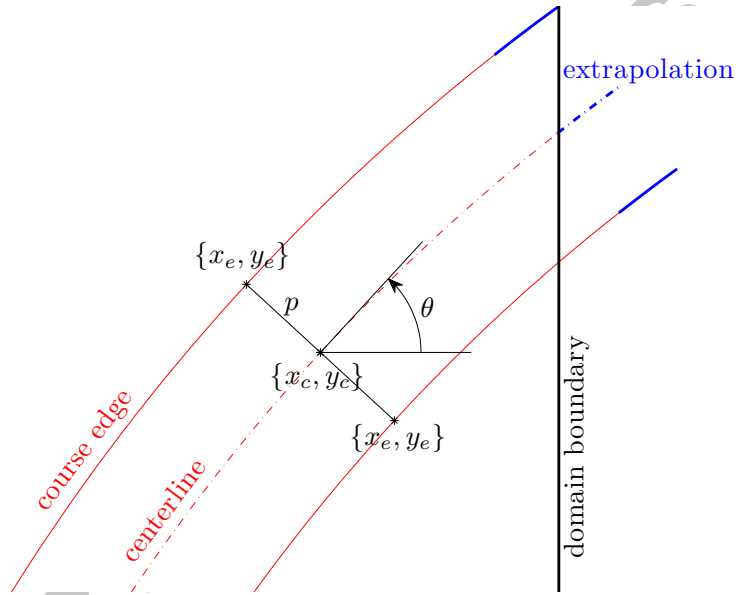


Fig. 3. Finite width course and path extrapolation

5 Results

First the results for a panel with a one-dimensional fiber angle distribution are presented. The differences between the optimization criteria are shown and the influence of periodic boundary conditions on the thickness distribution are demonstrated. For these criteria the corresponding thickness distributions resulting from discrete courses are also given. Second, the thickness distributions for two panels with a polynomial angle distribution in two directions are compared.

5.1 Unidirectional Fiber Angle Variation

To illustrate the differences between the various optimality criteria described in section 3, an example panel is analyzed which has the following linear angle variation in x-direction:

$$\theta(x, y) = -30 - 30 \frac{x}{l} \quad (21)$$

such that the fiber orientation is -30 degrees at the left side of the panel ($x = 0$) and -60 degrees at the right side of the panel ($x = l$). The length to width ratio of the panel is 3. This fiber angle distribution is only used for illustration of the presented theory and is not part of an optimized laminate definition.

5.1.1 Smeared Thickness Distribution

The thickness distribution of a panel for which the maximum thickness is minimized is shown in Fig. 4(a). The resulting thickness along the left and top edge is unity, indicating that there are no overlaps on these sides. The maximum thickness occurs in the lower right corner of the panel. The thickness distribution of a panel with maximized smoothness is presented in Fig. 4(b). When compared to the first panel the maximum thickness is increased by approximately 20 percent, while smoothness is improved by 40 percent. The smeared thickness for the combined objective with $w = 0.5$ is plotted in Fig. 4(c). Since both maximum thickness and smoothness are included in the objective function, the increase in maximum thickness is only 7 percent, while the improvement in smoothness is 30 percent when compared to the first panel. Finally a panel with periodic boundary conditions is shown in Fig. 4(d). The maximum thickness of this panel is more than 40 percent larger than the smallest maximum thickness, and also smoothness is decreased.

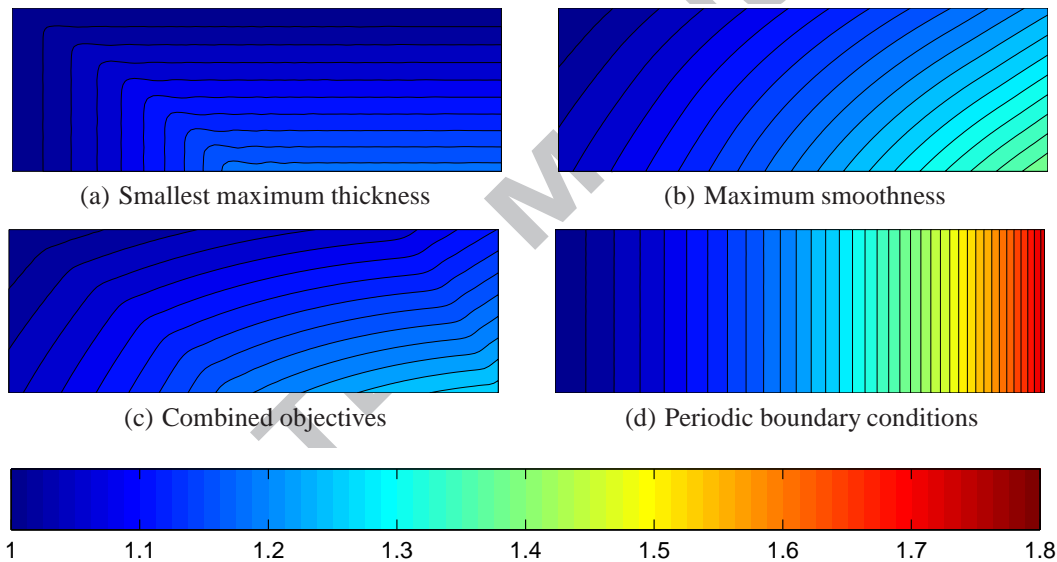


Fig. 4. Thickness distribution for various optimization criteria

5.1.2 Discrete Thickness Distribution

The discrete thickness distributions corresponding to the four smeared thickness distributions of Figs. 4 are shown in Figs. 5. The width of these courses was assumed to be $1/6$ of the panel width. The white areas in the figure indicate overlaps, while black regions are one layer thick.

Fig. 5(a) clearly shows the least amount of overlap. If a laminate with constant thickness was desired, the fiber paths obtained by this optimization can be used as basic paths and the overlaps could be eliminated by cutting individual tows on the sides of the courses. The smoothness of the laminate in Fig 5(b) is not readily apparent, until multiple plies are stacked on top of each other and staggered with respect to each other. The combined objective laminate of Fig. 5(c) is indeed in between the laminates of Figs. 5(a) and 5(b). Finally, the relatively large thickness build-up of the laminate with periodic boundary conditions is translated in large overlap areas, as shown in 5(d).

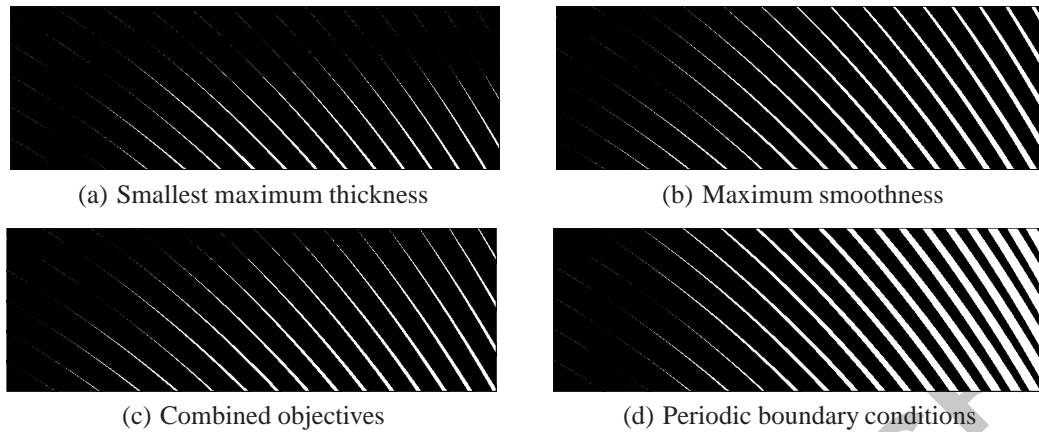


Fig. 5. Discrete thickness build-up (black = 1 layer, white = 2 layers)

5.2 Two Dimensional Fiber Angle Distributions

In Fig. 6 the smeared thickness for two different fiber angle distributions are presented. The graphs on the left correspond to a two-dimensional 2^{nd} order Lobatto polynomial and the graphs on the right correspond to a two-dimensional 3^{rd} order Lobatto polynomial, as described by Setoodeh [21]. The angle distributions shown represent one ply in a laminate that resulted from an optimization to match a given optimal lamination parameter distribution as closely as possible [21]. Due to the smaller number of design variables of the 2^{nd} order polynomial when compared to the 3^{rd} order polynomial (4 versus 9 variables), the latter better matched the given stiffness distribution. For more details on the laminate optimization the reader is referred to reference [21].

In Figs. 6(c) and 6(d) the thickness due to a uniform unit inflow is plotted. In both figures regions with values smaller than one are present, which indicates that in these areas there is no complete coverage of the surface. In other areas the thickness is larger than one, implying that overlaps are present. For the 2^{nd} order polynomial (Fig. 6(c)) the largest thickness is about five times larger than the thinnest region, while for the 3^{rd} order polynomial the thickest region is more than a million times thicker than the thinnest region. If no gaps are allowed and all thicknesses were scaled accordingly, this would result in a non-acceptable amount of overlap for the last variation.

Optimizing the thickness distribution in order to eliminate gaps and to minimize maximum thickness results in the smeared thicknesses shown in Figs. 6(e) and 6(f). The maximum thickness of the 2^{nd} order polynomial distribution is reduced by approximately 35 percent, while the amount of overlap for the 3^{rd} order polynomial distribution is reduced from one million to only 186 times maximum overlap.

Finally smoothness is maximized in Figs. 6(g) and 6(h) at the cost of increased thickness. For the second order polynomial the increase is thirty percent, while for the third order polynomial the increase is 145 percent.

Based on these results, the plate with the second order angle distribution would be preferred to the third order distribution, because the amount of overlap resulting from the latter is not practical from a manufacturability point of view. Due to the streamline analogy presented in this paper this observation can be made without having to fit discrete courses to the given fiber angle distribution. Once a configuration has been selected, the discrete courses matching one of the boundary conditions can be generated. In Fig. 7(a) the discrete courses for a uniform unit inflow are shown. The white areas indicate gaps, as was already predicted by the smaller the values smaller than one in the continuous thickness distribution of Fig. 6(c). Figs. 7(b) and 7(c) display the discrete thickness distributions for respectively the smallest maximum thickness and maximum smoothness conditions. These plots indicate that the maximum number of layers for the maximum smoothness distribution is indeed larger, while the difference in smoothness is not significant due to the small number of

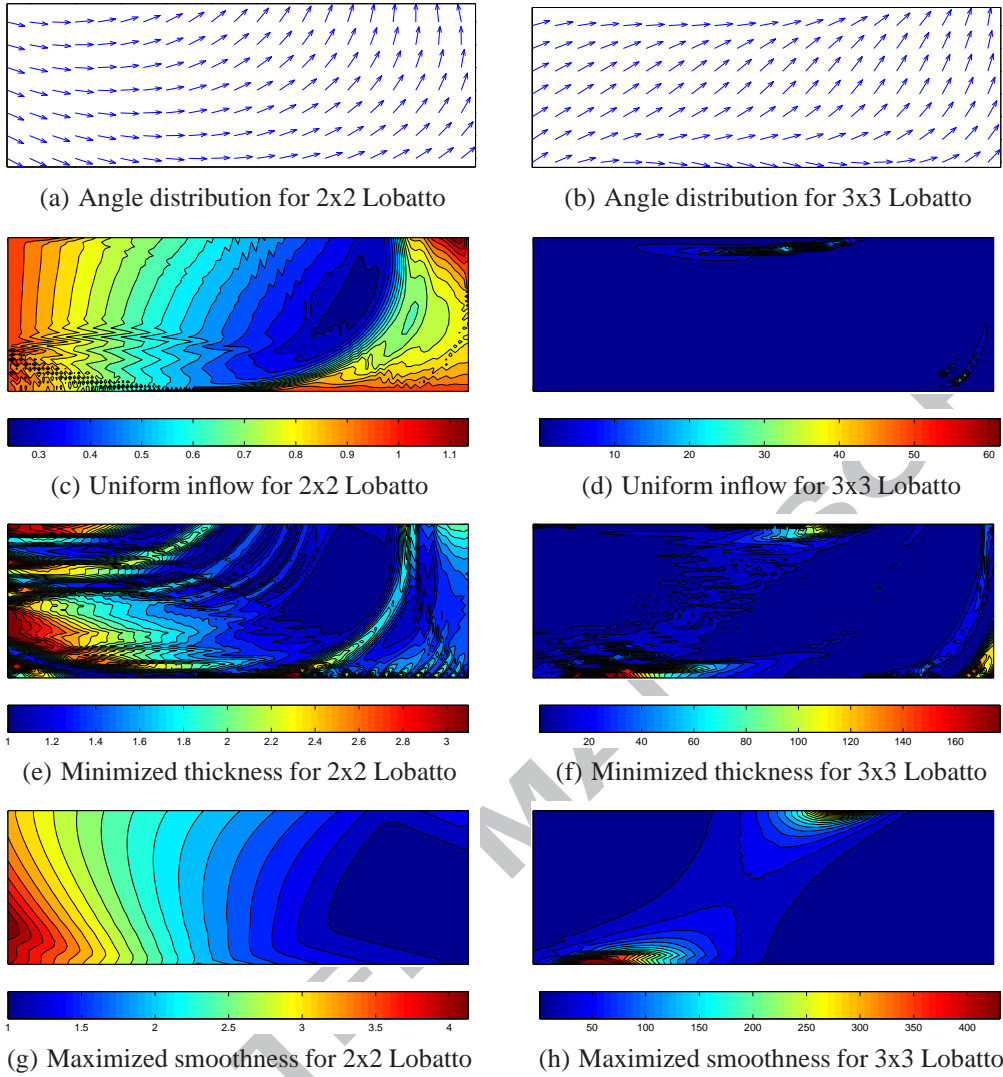


Fig. 6. Fiber angle and thickness distributions for 2^{nd} and 3^{rd} order Lobatto polynomials

layers in this ply.

The ply thickness optimization can be used to judge if it possible to obtain a constant-thickness ply by cutting tows on the outside of fiber courses. In the case of the 3x3 Lobatto variation the amount of overlap as predicted by the streamline analogy already indicates that too many overlaps would occur and that cutting tows is inefficient. The 2x2 Lobatto variation on the other hand has a maximum overlap of 6 layers, for which a local reduction of the course width by a factor 6 can result in a constant-thickness ply. Using fiber placement this is feasible, since the course width could be reduced from 32 to 5 or 6 tows locally in order to eliminate the overlaps. In other cases the thickness distribution might be fed back to the laminate optimization routine in order to include the effect of thickness buildup in the optimization, instead of assuming a constant thickness per ply.

6 Conclusions and Outlook

In this paper it was demonstrated that a stream line analogy can be successfully used to predict and influence the thickness distribution in a ply with variable fiber angles. Different objectives for optimization were considered, and in the future others, such as minimum volume, might be

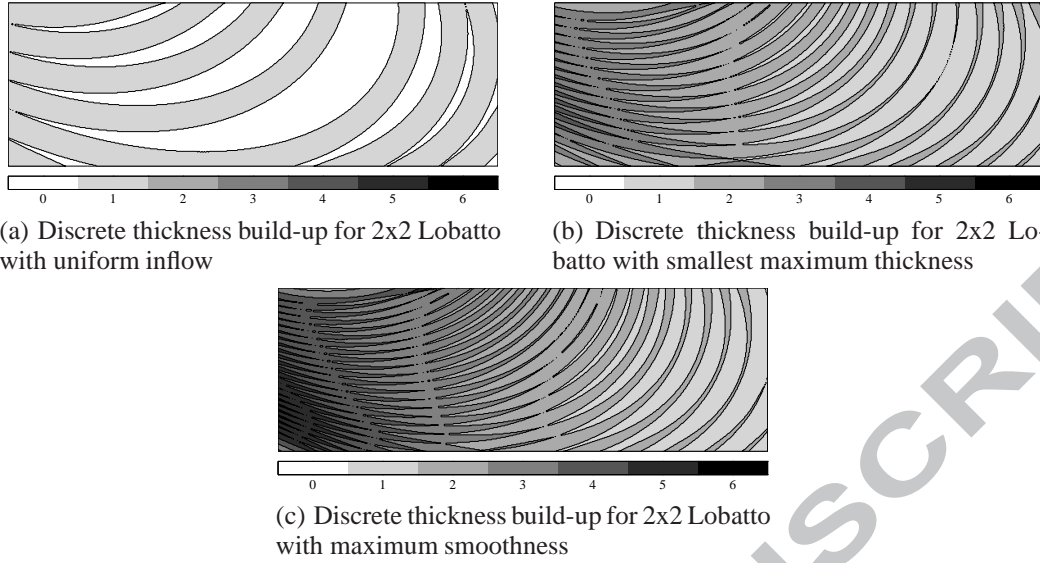


Fig. 7. Discrete thickness build-up

explored as well. The thickness information can be used to judge if a constant-thickness ply can be obtained, as constant thickness is often assumed in the optimization phase of variable-stiffness laminate design. Alternatively, the thickness optimization result can be included in the laminate optimization in order to take thickness buildup into account in the laminate design.

In addition to one-ply designs, the developed methods could be used to design complete laminates with both varying fiber angles and varying thickness. One approach would be to design the laminate using lamination parameters and thickness [7, 8, 21] as spatially varying design variables, and then as a post-processing step, multiple plies with varying fiber angles and their corresponding thickness distributions could be fit in order to match both the desired lamination parameters and thickness distribution as close as possible.

Finally, a similar method can be developed for curved surfaces in order to expand the applicability of the method.

Appendix A

The derivatives of the stream function are:

$$\begin{aligned}\Psi_{,x} &= -\Psi_{,n} \sin \theta = -t \sin \theta \\ \Psi_{,y} &= \Psi_{,n} \cos \theta = t \cos \theta\end{aligned}\quad (22)$$

The second derivatives of the stream function are:

$$\begin{aligned}\Psi_{,xy} &= -t \cos \theta \cdot \theta_{,y} - \sin \theta \cdot t_{,y} \\ \Psi_{,yx} &= -t \sin \theta \cdot \theta_{,x} + \cos \theta \cdot t_{,x}\end{aligned}\quad (23)$$

Continuity of the second derivatives of the stream function implies that $\Psi_{,xy} = \Psi_{,yx}$ so that:

$$\Psi_{,xy} - \Psi_{,yx} = t(\cos \theta \cdot \theta_{,y} - \sin \theta \cdot \theta_{,x}) - (\sin \theta \cdot t_{,y} + \cos \theta \cdot t_{,x}) = 0 \quad (24)$$

Rearrangement gives:

$$-\left(\cos\theta\frac{t_{,x}}{t} + \sin\theta\frac{t_{,y}}{t}\right) = -\sin\theta \cdot \theta_{,x} + \cos\theta \cdot \theta_{,y} \quad (25)$$

Using the following definitions:

$$\begin{aligned} \bar{n} &= \begin{Bmatrix} -\sin\theta \\ \cos\theta \end{Bmatrix} & \bar{\nabla}\theta &= \begin{Bmatrix} \theta_{,x} \\ \theta_{,y} \end{Bmatrix} \\ \bar{s} &= \begin{Bmatrix} \cos\theta \\ \sin\theta \end{Bmatrix} & \bar{\nabla}(\ln t) &= \begin{Bmatrix} t_{,x}/t \\ t_{,y}/t \end{Bmatrix} \end{aligned} \quad (26)$$

Eq. (25) can be written as:

$$-\bar{s}\bar{\nabla}(\ln t) = \bar{n}\bar{\nabla}\theta \quad (27)$$

References

- [1] Hyer MW, Charette RF. The use of curvilinear fiber format in composite structure design. In: Proceedings of the 30th AIAA/ASME/ASCE/AHS/ASC Structures, Structural Dynamics and Materials (SDM) Conference. New York, NY, USA. 1989.
- [2] Hyer MW, Lee HH. The use of curvilinear fiber format to improve buckling resistance of composite plates with central circular holes. *Composite Structures* 1991;18(3):239–261.
- [3] Nagendra S, Kodiyalam A, Davis JE, Parthasarathy VN. Optimization of tow fiber paths for composite design. In: Proceedings of the 36th AIAA/ASME/ASCE/AHS/ASC Structures, Structural Dynamics and Materials (SDM) Conference. New Orleans, LA, USA. 1995.
- [4] Waldhart C, Gürdal Z, Ribbens C. Analysis of tow placed, parallel fiber, variable stiffness laminates. In: Proceedings of the 37th AIAA/ASME/ASCE/AHS/ASC Structures, Structural Dynamics and Materials (SDM) Conference. Salt Lake City, UT, USA. 1996.
- [5] Parnas L, Oral S, Ceyhan U. Optimum design of composite structures with curved fiber courses. *Composites Science and Technology* 2003;63(7):1071–1082.
- [6] Hale R, Moon R, Lim K, Schueler K, Yoder A, Singh H. Integrated design and analysis tools for reduced weight, affordable fiber steered composites. Technical Report N00014-00-1-0415. University of Kansas Center for Research, Inc.. 2004.
- [7] Setoodeh S, Abdalla MM, Gürdal Z. Design of variable stiffness laminates using lamination parameters. *Composites, Part B: Engineering* 2006;37:301–309.
- [8] Abdalla MM, Setoodeh S, Gurdal Z. Design of variable stiffness composite panels for maximum fundamental frequency using lamination parameters. *Composite Structures* 2007; 81(2):283–291.
- [9] Tatting BF, Gürdal Z. Design and manufacture of elastically tailored tow placed plates. Technical report. 2002. NASA/CR-2002-211919.
- [10] Tatting BF, Gürdal Z. Automated finite element analysis of elastically-tailored plates. Technical report. 2003. NASA/CR-2003-212679.
- [11] Jegley DC, Tatting BF, Gürdal Z. Tow-steered panels with holes subjected to compression or shear loading. In: Proceedings of the 46th AIAA/ASME/AHS/ASC Structures, Structural Dynamics and Materials (SDM) Conference. Austin, TX, USA. 2005.
- [12] Huang J, Haftka RT. Optimization of fiber orientations near a hole for increased load-carrying capacity of composite laminates. *Structural and Multidisciplinary Optimization* 2005; 30(5):335–341.
- [13] Blom AW, Setoodeh S, Hol JMAM, Gürdal Z. Design of variable-stiffness conical shells for maximum fundamental eigenfrequency. *Computers and Structures* 2008;86(9):870–878.

- [14] Sun M, Hyer M. Use of material tailoring to improve buckling capacity of elliptical composite shells. *AIAA Journal* 2008;46(3):770–782.
- [15] Blom AW, Stickler PB, Gürdal Z. Optimization of a composite cylinder under bending by tailoring stiffness properties in circumferential direction. 2009 Article in press, doi:10.1016/j.compositesb.2009.10.004.
- [16] Alhajahmad A, Abdalla MM, Gürdal Z. Design tailoring for pressure pillowing using tow-placed steered fibers. *AIAA Journal of Aircraft* 2008;45(2):630–640.
- [17] Alhajahmad A, Abdalla MM, Gürdal Z. Optimal design of a pressurized fuselage panel with a cutout using tow-placed steered fibers. In: *Proceedings of the International Conference on Engineering Optimization*. Rio de Janeiro, Brazil. 2008 .
- [18] Blom AW, Tatting BF, Hol JMAM, Gürdal Z. Path definitions for elastically tailored conical shells. *Composites part B: engineering* 2008;Doi:10.1016/j.physletb.2003.10.071.
- [19] Wu KC, Gürdal Z, Starnes J. Structural response of compression-loaded, tow-placed, variable stiffness panels. In: *Proceedings of the 43rd AIAA/ASME/AHS/ASC Structures, Structural Dynamics and Materials (SDM) Conference*. Denver, CO, USA. 2002 .
- [20] Wu KC. Design and analysis of tow-steered composite shells using fiber placement. In: *Proceedings of the American Society for Composites 23rd Technical Conference*. Memphis, TN, USA. 2008 .
- [21] Setoodeh S, Blom AW, Abdalla MM, Gürdal Z. Generating curvilinear fiber paths from lamination parameters distribution. In: *Proceedings of the 47th AIAA/ASME/ASCE/AHS/ASC Structures, Structural Dynamics and Materials (SDM) Conference*. Newport, RI. 2006 .
- [22] The MathWorks, Inc. *Matlab Version 6.5R13 Documentation*. 2002.
- [23] Olhoff N. Multicriterion structural optimization via bound formulation and mathematical programming. *Structural Optimization* 1989;1:11–17.